Angle-resolved scattering: an effective method for characterizing thin-film coatings

Sven Schröder,[1,*] Tobias Herffurth,[1] Holger Blaschke,[2] and Angela Duparré[1]

[1]Fraunhofer Institute for Applied Optics and Precision Engineering, Albert-Einstein-Straße 7, 07745 Jena, Germany

[2]Laser Zentrum Hannover e.V., Hollerithallee 8, 30419 Hannover, Germany

*Corresponding author: sven.schroeder@iof.fraunhofer.de

Light scattered from interface imperfections carries valuable information about its origins. For single surfaces, light-scattering techniques have become a powerful tool for the characterization of surface roughness. For thin-film coatings, however, solving the inverse scattering problem seemed to be impossible because of the large number of parameters involved. A simplified model is presented that introduces two parameters: Parameter δ describes optical thickness deviations from the perfect design, and parameter β describes the roughness evolution inside the coating according to a power law. The new method is used to investigate structural and alteration effects of HR coatings for 193 nm, as well as laser-induced degradation effects in Rugate filters for 355 nm.   © 2010 Optical Society of America
   OCIS codes: 310.0310, 290.0290, 240.5770, 140.3330, 120.6660.

1. Introduction

For optical surfaces and coatings, light scattering from interface imperfections is typically seen as an unwanted effect. On the one hand, light scattering corresponds to a reduction of usable specular power and thus limits the throughput of an optical system. On the other hand, light scattered close to the specular direction reduces the image quality of optical components. However, despite these negative properties, scattered light also carries valuable information about its origins. This can be exploited to measure interface roughness or to detect surface and subsurface defects as well as bulk inhomogeneities. Compared to other characterization techniques, light-scattering measurements have some exclusive advantages: They are noncontact, nondestructive, fast, robust, and even large sample areas can be investigated [1]. Light-scattering techniques can even be integrated into fabrication processes or test environments.

At the Fraunhofer IOF, instruments for light-scattering measurements at various wavelengths have been developed, together with analysis techniques to link the scattering with the structural properties of surfaces, thin-film coatings, and bulk materials [1–3].

For optically smooth single surfaces, the theoretical models are rather simple and provide direct relationships between light scattering and roughness. For example, angle-resolved scattering is directly proportional to the surface power spectral density [4]. This is the basis for the measurement of surface roughness using light-scattering measurement and analysis. The method has recently become a standard procedure at IOF for inspecting large EUV mirror substrates before coating, with superior characteristics in terms of sensitivity, robustness, flexibility, and speed, as well as a direct link to the optical performance at the wavelength of application, 13.5 nm [5].

Unfortunately, the analysis of thin-film coatings is much more complicated because of the large number of parameters involved. Although tools for the prediction of multilayer scattering have been developed at Fraunhofer IOF, and successfully used for the

qualitative interpretation of measurement data, it was not possible to solve the inverse scattering problem. A first general strategy for modeling multilayer scattering was discussed in [6] to describe the roughness evolution models and coating parameters used to interpret measured data. In this paper, we present a new simplified approach modeling the scattering from multilayer coatings that enables information about structural and optical properties of thin-film coatings to be obtained using two simple and illustrative parameters.

2. Theoretical Background

A. Scattering from Multilayer Coatings

A number of scattering theories for multilayer coatings have been developed by Elson *et al.* [7], Bousquet *et al.* [8], Amra *et al.* [9], and others. All these theories are based on a vector perturbation approach by assuming the interface roughness to be small compared to the wavelength of light. Even though the derivations are quite different, they essentially lead to the same results. We follow the derivation of Bousquet *et al.* [8], and the corresponding treatment has been implemented into a software code at Fraunhofer IOF.

For a coating consisting of M layers and isotropic roughness (for the sake of simplicity), the angle-resolved scattering (ARS), defined as the power ΔP_s scattered into a small solid angle $\Delta\Omega_s$ normalized to that solid angle and the incident power P_i, can be calculated as [2,8]:

$$\mathrm{ARS}(\theta_s) = \frac{\Delta P_s(\theta_s)}{\Delta\Omega_s P_i} \propto \sum_{i=0}^{M}\sum_{j=0}^{M} F_i F_j^* \mathrm{PSD}_{ij}(f). \quad (1)$$

θ_s is the polar scattering angle with respect to the sample normal. The F_i are optical factors containing information about the optical properties of the perfectly smooth multilayer (design, layer thickness, dielectric functions, etc.) and the conditions of illumination as well as detection (illumination and detection angles, polarization, etc.). The roughness factors PSD_{ij} comprise the power spectral density functions (PSD) of all interfaces (for $i = j$) as well as their cross-correlation properties (for $i \neq j$). The relationship between scattering angles and spatial frequencies f is given by the grating equation. For normal incidence, $f = \sin\theta_s/\lambda$. The scattering geometry and the nomenclature used are shown in Fig. 1.

Equation (1) is the most general result for optical interference coatings, and can be seen as an exact forward solution to first order of the scattering problem if the interface roughness is sufficiently small compared to the wavelength of light ($\sigma/\lambda \ll 1$). The number of parameters required to model the ARS, however, is proportional to M^2. This makes it impossible to solve the inverse scattering problem and hence, to obtain information about the coating from scattering measurements. Therefore, we propose a simplified model.
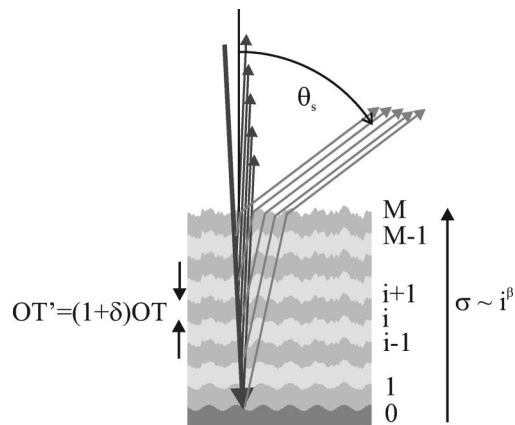

Fig. 1. Scattering geometry and nomenclature.

B. Simplified Modeling Procedure

The basic approach to reducing the number of parameters is to use physically meaningful models that describe the natural coupling of several parameters in real-world coatings. In the following, two such simplifications are presented in detail.

The first consideration is to assume that the multilayer might have an average deviation of the optical thickness from the perfect design, caused by an optical density or physical thickness other than expected. We therefore introduce the optical parameter δ that describes the average deviation of the optical layer thickness (OT) from the perfect design. For each layer, $\mathrm{OT}' = (1 + \delta)\mathrm{OT}$. This approximation, which assumes the thickness deviation to be constant throughout the multilayer, could be extended to include gradually increasing deviations, if necessary.

Another simplification is based on the observation that the evolution of the rms roughness of a single thin film with increasing thickness d can be described using a power law of the form $\sigma \sim d^\beta$ [10,11], where β is called the dynamic scaling exponent and is related to the fundamental growth process ($\beta = 0.5$: stochastic roughening; $\beta > 0.5$: rapid roughening; $\beta = 0$: saturated roughness, epitaxial growth, or perfect replication). Investigations of multilayers with increasing number of periods suggested that power laws also hold for thin-film stacks, hence, with i being the index of the interface, $\sigma(i) \propto i^\beta$. For thermal boat evaporated metal fluoride multilayers, β between 0.15 and 1.0 were observed [12]. For coatings fabricated using high-energy deposition processes such as magnetron sputtering, the linear growth theory [13] suggests β to be equal to 0.5. In the following, we simply refer to the generalized scaling exponent β as the roughness parameter.

However, PSDs of all interfaces, rather than just the corresponding rms roughness values, are required to model the angle-resolved scattering of a multilayer coating. Since the rms roughness is the square root of the integral of the PSD, β can be used to generate a set of PSDs based on one initial PSD by simply scaling the height of the PSD. The PSD of a

film usually can be decomposed into a substrate component and an intrinsic thin-film component [14]. Using an ABC-PSD model for the thin-film component with $PSD_i(f) = A_i/(1 + B^2f^2)^{(C+1)/2}$ and assuming parameters B and C to be constant throughout the stack it is straightforward to show that parameter $A_i(\beta) = aB^2(C-1)i^{2\beta}/2\pi$. The assumptions are justified as long as B and C only influence very high spatial frequency components that are not relevant for the scattering properties. The constant a can be determined by fitting the model PSD to a measured PSD of one arbitrary interface, which is the procedure used in this paper, or by using additional scatter data at other wavelengths or angles of incidence.

Following the considerations outlined above, the full set of M^2 parameters can be drastically reduced to only two parameters that are based on reasonable concepts and physically meaningful parameters. With the simplified model, the measured ARS of a given coating can be analyzed using the following procedure:

1. ARS measurement, at certain conditions (wavelength, angle of incidence) that do not have to be identical with, but should be close to, the conditions of application.
2. Determination of top-surface (or, alternatively, substrate) PSD. This can be done using atomic force microscopy (AFM), white light interferometry (WLI), angle-resolved light-scattering measurements at different wavelengths, angle of incidence, or other appropriate methods and combinations of different methods.
3. Definition of modeling start parameters: $\delta = 0$ (perfect design) and $\beta = 0$ (identical interfaces). Any *a priori* knowledge can be put into the model at this point.
4. ARS modeling using Eq. (1) with parameters δ and β.
5. Comparison of measured and modeled ARS, refinement of parameters δ and β, and remodeling (back to step 4).

The final result is a comprehensive model of the coating properties comprising (i) the top-surface (or substrate) roughness, (ii) the roughness evolution inside the coating (β), (iii) the theoretical design, and (iv) the average deviation from the theoretical design (δ). Hence, all relevant information about the optical and structural properties of the real multilayer is obtained. As will be demonstrated in Section 4, variations of the two parameters have significantly different impacts on the modeling results. While variation of β primarily influences the resonant scattering close to the specular directions, variation of δ influences the thin-film interference properties. This naturally occurring decoupling is a fundamental basis for the robustness of the modeling procedure and the uniqueness of the results.

3. Experimental Setups

Several instruments for light-scattering measurements that have been developed at the Fraunhofer IOF that cover a wide range of wavelengths, from the visible extending up to the IR [15], and down to the deep UV (DUV) [16] and extreme UV spectral regions [17]. In the design of our instruments, special care has been taken to achieve high dynamic ranges and low noise equivalent scattering levels, which are limited in most cases only by unavoidable Rayleigh scattering in the laboratory atmosphere. This precaution is essential in order to also investigate high-quality, low-scattering samples such as superpolished substrates. Table 1 gives an overview of the wavelengths available for angle-resolved scattering measurements and the performance achieved at IOF. In addition, several instruments that are consistent with the international standard ISO 13696 [15,18], a table-top system for light scattering and roughness characterization close to manufacturing processes [19], and a light-scattering based roughness sensor [20] have been developed.

For the scattering measurements at 193 nm, the DUoSTAR instrument (Deep UV Scattering, Transmittance, and Reflectance) was used in ARS mode. This instrument, which is based on an ArF* excimer laser as light source and a precision double-goniometer for ARS measurements, is described in detail in [6,16].

For ARS measurements at 325 nm, the ALBATROSS instrument (3D) Arrangement for Laser-Based Transmittance, Reflectance, and Optical Scatter Measurement) for light-scattering measurements in the UV–VIS–IR spectral ranges was used. The instrument is located in a class 10000 clean room

Table 1. Wavelengths, Associated Dynamic Ranges, and Noise-Equivalent ARS Levels of Instruments for Angle-Resolved Scattering Measurements at Fraunhofer IOF

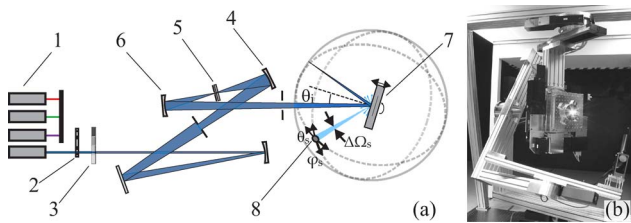| Spectral Range	Wavelength	Dynamic Range (orders of magnitude)	Noise-Equivalent ARS (Sr^{-1})
EUV	13.5 nm	7	10^{-4} (vacuum)
DUV, VUV	193 nm, 157 nm	12	10^{-7} (vacuum) 10^{-6} (nitrogen purge)
UV-VIS	325 nm, 442 nm, 532 nm, 633 nm	up to 15	down to 10^{-8}
NIR-IR	1064 nm, 4.5 μm, 10.6 μm	up to 10	down to 10^{-5}
Currently being implemented: VIS-NIR	650 nm, 690 nm, 780 nm, 808 nm, 850 nm	target: >11	target: 10^{-6}

Fig. 2. (Color online) ALBATROSS instrument for ARS measurement in UV–VIS–IR spectral range. (a) Schematic. (b) Photograph showing a sample (center) mounted onto the sample positioning system, as well as the detector and 3D goniometer.

under laminar flow boxes (effective clean room <100). The setup is shown schematically in Fig. 2(a): (1) Several lasers are currently implemented as light sources, including a HeCd laser for 325 nm or 442 nm, a 2ω-Nd:YAG laser for 532 nm, a HeNe laser for 633 nm, and a Nd:YAG laser for 1064 nm. (2) A chopper is used to allow for lock-in amplification. (3) Neutral density filters are used to adjust the incident power according to the current scattering signal. Switching between different attenuators is essential to achieve the required dynamic range between the power of the incident beam and the low-level light scattering. (4) A spherical mirror coated with protected aluminum is used to focus the beam onto (5) a pinhole (diameter ~100 μm) that acts as spatial filter. The pinhole is then imaged by (6) a spherical mirror over (7) the sample onto (8) the detector aperture. Baffles at certain positions are introduced in order to block stray light from the beam preparation system. Since the spatial filter is based on metal mirrors, additional wavelengths in the UV–VIS–IR spectral range can easily be implemented without changing optical components.

The sample (7) is located on a positioning system that can be moved and rotated to adjust the irradiated position on the sample, as well as the angle of incidence. Plane or curved samples with diameters ranging from a few millimeters up to 670 mm can be mounted. Typical illumination spot diameters at the sample position are between 1 mm and 5 mm although focusing to about 50 μm is also possible depending on the application. Typical irradiances in the sample are on the order of 500 mW/cm^2.

The detector (8), which is based on a side-on photomultiplier tube (PMT), can be scanned within the entire sphere around the sample. This enables the 3D light-scattering distribution to be measured in order to investigate out-of-plane scattering or anisotropic samples. The diameter of the aperture in front of the PMT defines the detector solid angle $\Delta\Omega_s$. Aperture diameters between 0.5 and 5 mm are used depending on the specific requirements regarding sensitivity, speckle reduction, and near-angle limit.

Calibration of ARS measurements is performed either by measuring the incident power and the detector solid angle directly, or by measuring the scattering of a Spectralon diffuse reflectance standard. Usually, both methods usually are applied to cross-

check calibrations at different intensity levels or linearity.

Up to 15 orders of magnitude dynamic range are achieved for light-scattering measurements in the UV–VIS spectral range, depending on the wavelength. The performance of the instrument thus allows a wide range of samples to be investigated, extending from superpolished substrates, thin-film coatings, and optical materials to nanostructured and technically rough surfaces. Figure 2(b) is a photograph of the instrument showing the sample positioning and detector systems.

The dominant sources of uncertainty in light-scattering measurements using goniometric instruments are the effective size of the detector solid angle, fluctuations in the output power of the laser, the transmittances of the attenuation filters as well as shot noise and excess noise of the photomultiplier tube. Because of the large dynamic range required, linearity is of crucial importance, and it is, therefore, checked regularly by measuring overlapping ARS curves with different filter positions. The final relative uncertainty of ARS measurements following from error propagation is about 10%. For low-scattering samples with total scattering levels on the order of 10^{-5}, this means an absolute uncertainty of as low as 1 ppm.

4. Application to Thin-Film Coatings

A. Highly Reflective Coating for 193 nm

Thin-film coatings for 193 nm in the DUV spectral range are of crucial importance for applications in optical microlithography and material processing. Metal fluorides are used as coating materials because of their low DUV absorption, and thermal boat evaporation is still the principal deposition method used in order to maintain sufficient stochiometric properties.

Unfortunately, in contrast to other deposition processes, unassisted thermal evaporation leads to columnar growth. This results in considerable amounts of interface roughness and scattering losses as well as adsorption of water in the porous film structure. Questions regarding the influence of substrate or thin-film roughness or optical thickness errors often arise. Angle-resolved scattering measurements and application of the modeling procedure described in Subsection 2.B provide simple answers to these questions.

A highly reflective quarter-wave stack for 193 nm with 20 periods of AlF$_3$/LaF$_3$ pairs was deposited by thermal boat evaporation onto superpolished fused silica substrates ($\sigma = 0.34$ nm, AFM 10 × 10 μm^2).

As discussed in Section 2, an initial PSD of the coating is required to determine the constant a of the scaling approach that is used to determine the absolute PSDs of all interfaces. For this purpose, AFM in 1 × 1 μm^2, 10 × 10 μm^2, and 50 × 50 μm^2 scan areas was performed to measure the top-surface roughness. An AFM Veeco D3100 was used with single crystalline silicon tips in the Tapping Mode™.
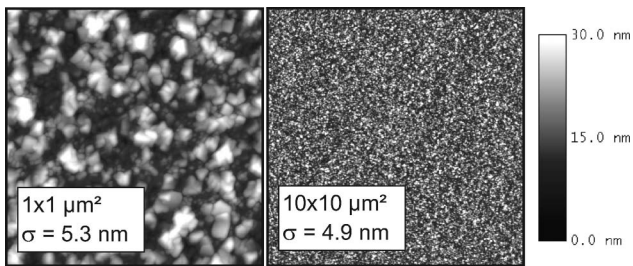
Fig. 3. Atomic force microscopy top-surface images of HR coating for 193 nm in 1×1 μm^2 and 10×10 μm^2 scan areas together with the corresponding bandwidth-limited rms roughness values.

Two typical top-surface AFM images are shown in Fig. 3. Single PSDs calculated for each scan were combined to a master PSD by weighted averaging as described in Ref. [21]. It should be noted that the procedure could also be applied based on substrate roughness data before coating.

ARS measurements were performed at 193 nm at near-normal incidence using the instrumentation developed at Fraunhofer IOF and described in [6,16]. Measurement and modeling results are shown in Fig. 4.

The measured curves exhibit a distinct peak at 0°, corresponding to the direction of specular reflection, as well as typical shoulders and ripples that can be explained by interference effects of waves scattered at different interfaces within the coating. The total backscattering calculated by numerical integration of the ARS according to ISO 13696 [18] is 2.8%.

The modeling results shown in Fig. 4(a) reveal that varying β but leaving δ constant ($\delta = 0$, perfect design) only influences the heights of the shoulders of the modeled curves. Based on the uncertainty in the ARS measurements (16%) and of the initial PSD (approximately 20%), the uncertainty for the determination of β is 0.3. This level is sufficient to identify the fundamental roughening regimes. The best fit for $\beta = 1$ indicates that the inner interfaces are much smoother than expected from the top-surface AFM data, or equivalently, that the coating exhibits a rapid roughening from interface to interface. Therefore, the parameter β provides a simple measure of the impact of substrate roughness and intrinsic thin-film roughness on the structural properties of the coating. It should be emphasized that only light-scattering measurements can provide such information about buried interfaces on a nondestructive basis.

In the next step, the modeling procedure is performed by varying δ but now leaving $\beta = 1$ constant. The results shown in Fig. 4(b) illustrate that this merely shifts the angular position of the wings. A more detailed analysis reveals that the wings are caused by resonant scattering, the constructive interference of light scattered from different interfaces within the coating. The angular position of the wings is thus associated with the center wavelength and the bandwidth of the coating. The best fit achieved for $\delta = 0.030 \pm 0.005$ indicates a deviation of 3% of
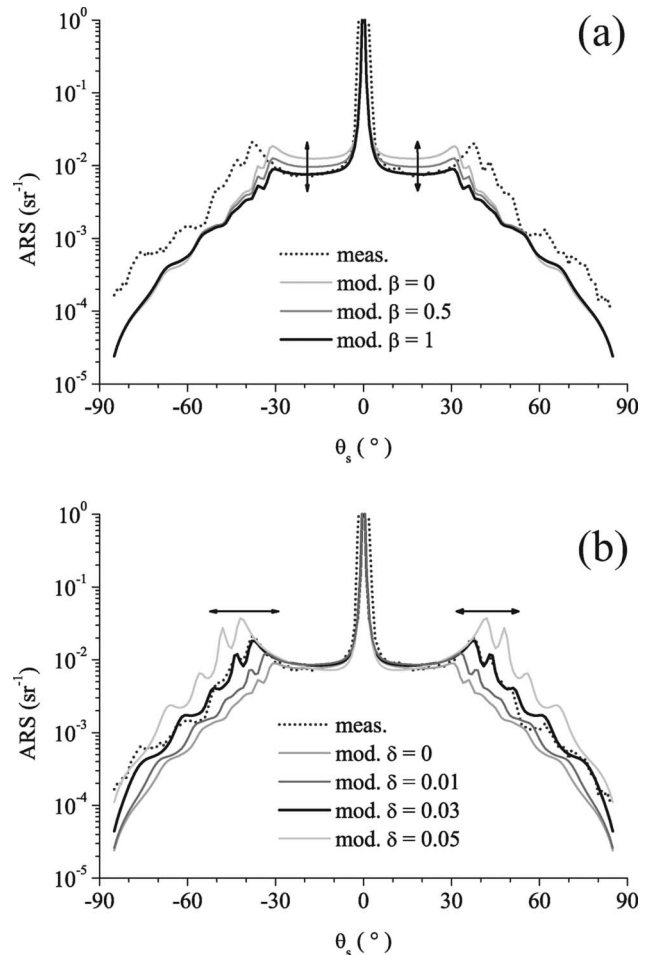

Fig. 4. Angle-resolved scattering of HR coating for 193 nm. Measurement (meas.) results obtained at 193 nm and modeling (mod.) results by varying (a) the roughness parameter and (b) the optical parameter.

the average optical thickness of each layer from the perfect quarter-wave design. This result is directly correlated to a spectral shift in the peak reflectance of the mirror, which is a well-known effect for porous coatings. A shift of $\Delta\lambda_c = \lambda_c\delta \approx 6$ nm toward longer wavelengths could be predicted, which was found to be in good agreement with spectral reflectance measurements (Lambda 900, PerkinElmer).

The final modeling curve for $\beta = 1$, $\delta = 0.03$ is in almost perfect agreement with the measurement result obtained at 193 nm. This demonstrates the accuracy of both the measurements and the modeling procedures. When a model has been established and proven to be valid by comparison with experimental results, the scattering properties also can be predicted for other conditions of application, as discussed in [6]. For the present coating, we can predict a total backscattering of as low as 1.4% if we assume the same roughness properties but accurate film thickness.

It is important to note that there is no coupling between the two parameters of the simplified model. This property, provided by the nature of multilayer

scattering and optical interference, is essential for the uniqueness of the solution of the reverse engineering procedure. It is expected to be valid in general for high-quality optical standard coatings such as quarter-wave stacks. It was not clear so far, however, whether the method can be applied to other types of thin-film coatings. In Section 4.B, we attempt to apply the modeling technique to Rugate notch filters.

B. Rugate Film after Laser-Damage Test

Rugate films have been demonstrated by the Laser Zentrum Hannover (LZH) to be a top candidate for optical coatings with substantially enhanced laser stability compared to standard stacks [22]. Instead of stacks of different material layers with finite thickness leading to a binary steplike variation of the dielectric function inside the coating, Rugate filters consist of material mixtures to achieve gradually changing (sinusoidal) dielectric property profiles inside the coatings.

For highly reflective mirrors, it has been demonstrated that the damage threshold of Rugate filters can exceed that of a standard multilayer coating by a factor of 10. Investigations at 1064 nm revealed that laser-induced damage in Rugate films induced by high-power irradiation often occurs in the form of alterations of the optical properties inside the films, compared to the well-known ablation effects of standard stacks.

The ARS analysis procedure presented in Section 2 has been demonstrated to be sensitive to both interface roughness and to alterations of optical thickness properties. Although the scattering model was developed for conventional multilayer stacks, the physical origins of scattering, fluctuations of optical and structural properties, should be similar for Rugate films.

A Rugate notch filter for 355 nm was fabricated at LZH using ion-beam sputtering (IBS). Laser-induced damage threshold S-on-1 tests were then performed at LZH at 355 nm by irradiating different sample positions on a regular matrix (effective beam diameter 250 μm, repetition rate 10 Hz, effective pulse duration 11 ns). Following the laser-damage tests, light-scattering measurements were performed at 325 nm at Fraunhofer IOF, using the instrumentation described in Section 3.

First, a scatter mapping was performed by scanning the entire sample surface and measuring the scattering into a fixed scatter angle of 45°. The illumination spot diameter was adjusted to 0.15 mm. The scatter map shown in Fig. 5 clearly reveals damaged and undamaged irradiation sites on the rather homogeneous intrinsic scatter of the nonirradiated areas. Therefore, this simple but sensitive technique seems to be very powerful for the automatic post evaluation of laser-damage tests, or even for correlating sample properties before and after irradiation in order to check for possible damage precursors.

In addition, different types of defects can be identified: (i) sharp defects (small dots in scatter map)
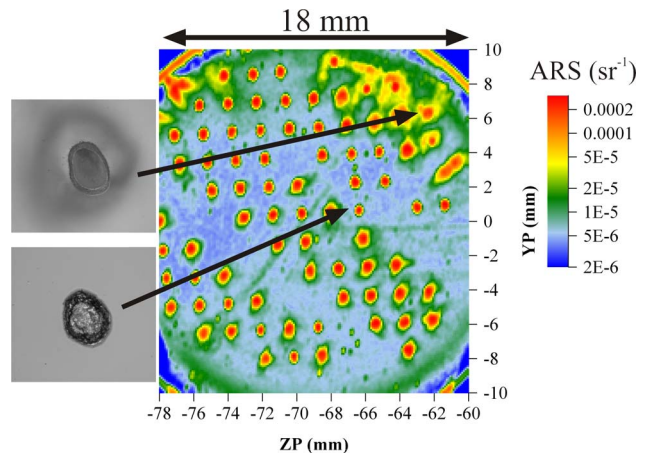

Fig. 5. (Color online) Scatter map at 325 nm revealing different types of defects and DIC images (field of view 0.85×0.85 mm^2) of two different defects indicating surface and bulk effects.

corresponding to pure surface defects, and (ii) defects surrounded by halos. The differential interference contrast (DIC) images (field of view 0.85×0.85 mm^2) in Fig. 5 indicate that the halos correspond to altered optical properties in the bulk of the film caused by intense laser irradiation.

In order to investigate these alteration effects in more detail, angle-resolved scattering measurements were performed at 325 nm at several positions near a damaged site. The measurement positions and the corresponding ARS curves are shown in Fig. 6(a).

The ARS curves clearly reveal a substantially higher scattering at the center of the defect as compared to the intrinsic scattering of the film; the corresponding total backscattering increases from only 0.4% in the undamaged region to as much as 25% on the defect site. In particular, the enhanced near-angle scattering indicates a surface-dominated effect. The fluctuations of the ARS curves can be explained by statistical effects caused by the focused illumination [23,24].

More surprisingly, it can be clearly observed in Fig. 6(a) that the intrinsic scattering of the Rugate film at an outer, nonirradiated position (lowest curve) exhibits peaks near 15° from the specular direction. This indicates similar physical origins of scattering of the Rugate films as for standard multilayer coatings. Furthermore, the angular positions of the peaks shift from 15° to 20° as the position of investigation approaches the defect site. This shift of the resonant scattering peak indicates that the halo, in fact, originates from the bulk of the film and the optical thickness of the coating increases towards the defect site. A possible explanation for the alteration of the optical thickness is the high thermal load during irradiation.

Until now, only qualitative interpretations of the observations for the Rugate film could be given based on the results of Subsection 4.A. It previously was not possible to apply the modeling procedure to gradient index films, because the scattering calculation still has been based on Eq. (1), which requires parameters
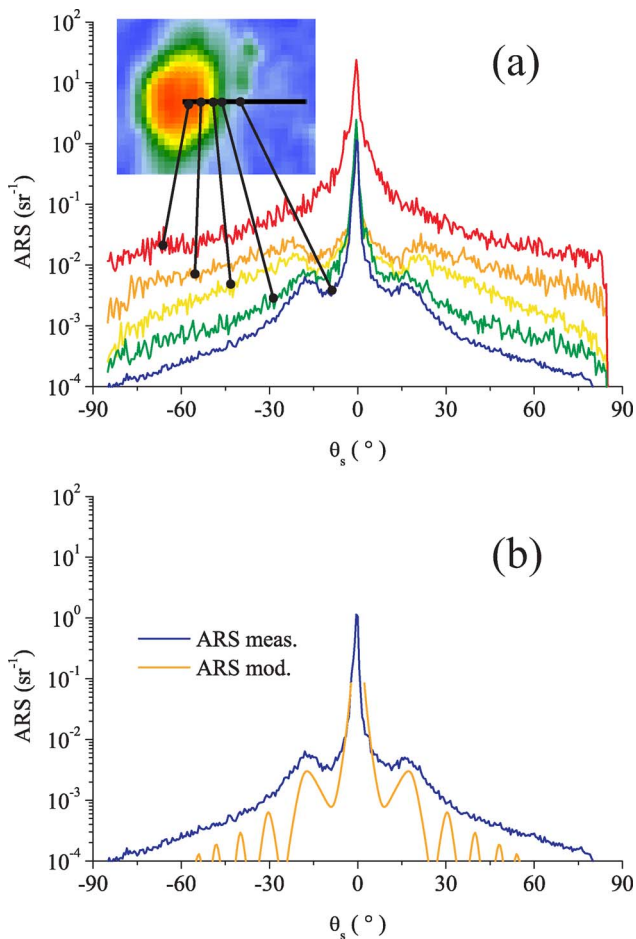
Fig. 6. (Color online) Angle-resolved scattering of a Rugate film. (a) Measured at 325 nm at several positions near a defect site caused by laser-induced damage. (b) Results of ARS modeling compared to measured curve.

like film thickness and interface roughness as input parameters. We solved this issue by discretization of the continuous index profile into 700 single layers with about 200 different dielectric functions. This challenging task requires further optimization of the calculation routine. However, we were able to model an ARS curve for the Rugate film in an undamaged region.

The results shown in Fig. 6(b) demonstrate that the modeling exactly predicts the presence as well as the position of the resonant peaks near 15°. This indicates that the scattering of Rugate films is caused by similar mechanisms as are in effect for standard stacks. The strong oscillations in the modeled curve can be explained by interference effects as a result of the artificial discretization. The natural deviations of the periodicity of the real coating lead to a suppression of these effects.

To the best of our knowledge, the result presented in this section is the first demonstration of modeling the angle-resolved scattering of a gradient index coating. In order to achieve adequate agreement, particularly regarding the absolute heights of the curves, however, a substrate roughness higher than

the top-surface roughness of the coating had to be assumed, corresponding to $\beta < 0$, which indicates a smoothing effect. Although this seems to be a reasonable assumption, considering the smoothing properties of high energetic deposition techniques like IBS, more detailed investigations of the scattering in Rugate films is required.

Nevertheless, it is already possible to analyze the shift of the resonant peak quantitatively. It has been found that even small optical thickness errors of as low as 0.3% result in significant changes of the angular position of the resonant peak of 1.5°, which can be explained by the small bandwidth of the filter. Therefore, the measured curves indicate small alterations in the optical thickness in the vicinity of the laser-induced defect, most likely caused by the thermal load during irradiation and defect formation. It could be very interesting to implement the scattering measurement and analysis procedure within a laser-damage test setup in order to investigate laser-induced degradation, even during irradiation.

5. Summary and Conclusion

Light-scattering measurement and analysis constitute a powerful approach to the characterization of surfaces and thin-film coatings. A number of tools for the measurement of the total and angle-resolved scattering at various wavelengths have been developed at Fraunhofer IOF. However, so far, the quantitative analysis of measurement results had been confined to single surfaces for which light scattering enables the surface roughness to be measured directly. For multilayer coatings, the large number of parameters involved prohibited obtaining quantitative information about the coating from scattering measurements.

A new simplified modeling procedure has been presented in this paper. The method is based on two simple parameters to describe the roughness evolution from interface to interface inside the coating as well as the deviations of the optical thickness from the perfect design. Illustrative information are obtained about the structural and optical properties of thin-film coatings using a reverse engineering procedure. Depending on the *a priori* knowledge available, the method could be adapted to detect other relevant parameters as well.

The method was applied to analyze highly reflective mirrors at 193 nm, as well as after a Rugate filter at 355 nm laser-damage tests. For the DUV coating, rapid roughening of the multilayer as a result of columnar growth and an optical thickness deviation of 3% caused by water adsorption were detected. For the Rugate filter, the simulation approach had to be modified substantially in order to model gradient index films. The first results clearly indicate that the scattering of Rugate films is induced by mechanisms similar to those in standard stacks. The investigation of film areas close to damage sites revealed increases of as low as 0.3% of the optical thickness compared to undamaged regions as a result of

thermal load during damage formation. The method could, therefore, be very useful for the sensitive characterization of laser-induced degradation, even during irradiation.

References

1. S. Schröder and A. Duparré, "Finish assessment of complex surfaces by advanced light scattering techniques," Proc. SPIE **7102**, 71020F (2008).
2. A. Duparré, "Scattering from surfaces and thin films," in *Encyclopedia of Modern Optics*, B. D. Guenther, D. G. Steel, and L. Bayvel, eds. (Elsevier, 2004).
3. S. Schröder, M. Kamprath, A. Duparré, A. Tünnermann, B. Kühn, and U. Klett, "Bulk scattering properties of synthetic fused silica at 193 nm," Opt. Express **14**, 10537–10549 (2006).
4. J. Stover, *Optical Scattering-Measurement and Analysis*, 2nd ed. (SPIE Press, 1995).
5. M. Trost, S. Schröder, T. Feigl, and A. Duparré, "Influence of the substrate finish and thin film roughness on the optical performance of Mo/Si multilayers," Appl. Opt. 50, C148–C153 (2011).
6. S. Schröder, A. Duparré, and A. Tünnermann, "Roughness evolution and scatter losses of multilayers for 193 nm optics," Appl. Opt. **47**, C88–C97 (2008).
7. J. M. Elson, "Diffraction and diffuse scattering from dielectric multilayers," J. Opt. Soc. Am. **69**, 48–54 (1979).
8. P. Bousquet, F. Flory, and P. Roche, "Scattering from multilayer thin films: theory and experiment," J. Opt. Soc. Am. **71**, 1115–1123 (1981).
9. C. Amra, "Light scattering from multilayer optics. I. Tools of investigation," J. Opt. Soc. Am. A **11**, 197–210 (1994).
10. R. Messier, "Toward quantification of thin film morphology," J. Vac. Sci. Technol. A **4**, 490–495 (1986).
11. W. M. Tong and R. S. Williams, "Kinetics of surface growth: phenomenology, scaling, and mechanisms of smoothening and roughening," Annu. Rev. Phys. Chem. **45**, 401–438 (1994).
12. S. Schröder, H. Uhlig, A. Duparré, and N. Kaiser, "Nanostructure and optical properties of fluoride films for high-quality DUV/VUV optical components," Proc. SPIE **5963**, 231–240 (2005).
13. D. G. Stearns, "Stochastic model for thin film growth and erosion," Appl. Phys. Lett. **62**, 1745–1747 (1993).
14. J. Ferré-Borrull, A. Duparre, and E. Quesnel, "Procedure to characterize microroughness of optical thin films: application to ion-beam-sputtered vacuum-ultraviolet coatings," Appl. Opt. **40**, 2190–2199 (2001).
15. S. Schröder, S. Gliech, and A. Duparré, "Sensitive and flexible light scatter techniques from the VUV to IR regions," Proc. SPIE **5965**, 424–432 (2005).
16. S. Schröder, S. Gliech, and A. Duparré, "Measurement system to determine the total and angle-resolved light scattering of optical components in the deep-ultraviolet and vacuum-ultraviolet spectral regions," Appl. Opt. **44**, 6093–6107 (2005).
17. S. Schröder, T. Herffurth, M. Trost, and A. Duparré, "Angle-resolved scattering and reflectance of extreme-ultraviolet multilayer coatings: measurement and analysis," Appl. Opt. **49**, 1503–1512 (2010).
18. "Optics and optical instruments-test methods for radiation scattered by optical components," ISO 13696:2002 (International Organization for Standardization, 2002).
19. A. Finck, M. Hauptvogel, and A. Duparré, "Instrument for close-to-process light scatter measurements of thin film coatings and substrates," submitted to Appl. Opt.
20. T. Herffurth, S. Schröder, M. Trost, and A. Duparré, "Roughness measurement of ultra precision surfaces using light scattering techniques and analysis," in *Optical Fabrication and Testing*, OSA Technical Digest (CD) (Optical Society of America, 2010), paper OTuA5.
21. A. Duparré, J. Ferre-Borrull, S. Gliech, G. Notni, J. Steinert, and J. M. Bennett, "Surface characterization techniques for determining the root-mean-square roughness and power spectral densities of optical components," Appl. Opt. **41**, 154–171 (2002).
22. M. Jupé, M. Lappschies, L. Jensen, K. Starke, and D. Ristau, "Laser-induced damage in gradual index layers and Rugate filters," Proc. SPIE **6403**, 64031A (2006).
23. P. Bakucz, R. Krüger-Sehm, S. Schröder, A. Duparré, and A. Tünnermann, "Wavelet Filterung von fraktalen Oberflächen," Technisches Messen **75**, 339–345 (2008).
24. E. L. Church, "Statistical effects in the measurement and characterization of smooth scattering surfaces," Proc. SPIE **511**, 18 (1984).